

Spatiotemporal dynamics of human object recognition processing: An integrated high-density electrical mapping and functional imaging study of “closure” processes

Pejman Sehatpour,^{a,b} Sophie Molholm,^a Daniel C. Javitt,^{a,c} and John J. Foxe^{a,c,*}

^aThe Cognitive Neurophysiology Laboratory, Nathan S. Kline Institute for Psychiatric Research, Program in Cognitive Neuroscience and Schizophrenia, 140 Old Orangeburg Road, Orangeburg, NY 10962, USA

^bFerkauf Graduate School Of Psychology, Albert Einstein College of Medicine, 1300 Morris Park Avenue, Bronx, NY 10461, USA

^cProgram in Cognitive Neuroscience, Department of Psychology, The City College of the City University of New York, North Academic Complex, 138th St. and Convent Avenue, New York, NY 10031, USA

Received 27 April 2005; revised 3 July 2005; accepted 27 July 2005
Available online 15 September 2005

Humans are capable of recognizing objects, often despite highly adverse viewing conditions (e.g., occlusion). The term “perceptual closure” has been used to refer to the neural processes responsible for “filling-in” missing information in the visual image under such conditions. Closure phenomena have been linked to a group of object recognition areas, the so-called lateral–occipital complex (LOC). Here, we investigated the spatiotemporal dynamics of perceptual closure processes by coregistering data from high-density electrical recordings (ERPs) and functional magnetic resonance imaging (fMRI) while subjects participated in a perceptual closure task. Subjects were presented with highly fragmented images and control scrambled images. Fragmented images were calibrated to be ‘just’ recognizable as objects (that is, perceptual closure was necessary), whereas the scrambled images were unrecognizable. Comparison of responses to these two stimulus classes revealed the neural processes underlying perceptual closure. fMRI revealed an object recognition system that mediates these closure processes, the core of which consists of the LOC regions. ERP recordings resulted in the well-characterized N_{CL} component (for negativity associated with closure), a robust relative negativity over bilateral occipito-temporal scalp that occurs in the 230–400 ms timeframe. Our investigations further revealed an extended network of dorsal and frontal regions, also involved in perceptual closure processes. Inverse source analysis showed that the major generators of N_{CL} localized to the identical regions within LOC revealed by the fMRI recordings and detailed the temporal dynamics across these LOC regions including interactions between LOC and these other nodes of the object recognition circuit.

© 2005 Elsevier Inc. All rights reserved.

Introduction

One critical and highly adaptive aspect of human object recognition processes is our seemingly effortless ability to identify objects even when only partial, and often very sparse visual information is presented to the observer. The neural processes responsible for filling-in of missing information that enables eventual object recognition under partial viewing conditions (e.g., fog, partial occlusion, camouflage, poor lighting) have come to be referred to as “perceptual closure” processes (e.g., Bartlett, 1916; Snodgrass and Feenan, 1990; Foley et al., 1997). The present study uses the excellent temporal resolution of high-density electrical recordings in combination with the precise spatial localization abilities of functional imaging to investigate the spatiotemporal dynamics of these perceptual closure processes.

In the past decade, both functional imaging and electrophysiological studies have been used separately to investigate the neural processes responsible for basic object recognition. Functional imaging studies have revealed a cluster of regions within the so-called ventral visual stream that play an important role in cue-invariant object recognition (e.g., Malach et al., 1995; Kanwisher et al., 1997; Grill-Spector et al., 1998; Haxby et al., 1999). This cluster of regions is known as the lateral–occipital complex (LOC). The LOC is situated at the lateral and ventral aspects of the occipital lobe, which includes dorsal–lateral–occipital lobe close to area MT/V5 and ventral fusiform (Malach et al., 1995; Lerner et al., 2001). To our knowledge, only a single functional imaging study, which used positron emission tomography (PET), has directly investigated perceptual closure processes, and this study suggested that closure processes were also carried out within regions of the LOC (Gerlach et al., 2002). Two other related studies (Op de et al., 2000; Denys et al., 2004) have also shown activation in the regions of LOC while presenting degraded and scrambled shapes, presumably resulting from the activity of closure processes,

* Corresponding author. The Cognitive Neurophysiology Laboratory, Nathan S. Kline Institute for Psychiatric Research, Program in Cognitive Neuroscience and Schizophrenia, 140 Old Orangeburg Road, Orangeburg, NY 10962, USA. Fax: +1 845 398 6545.

E-mail address: foxe@nki.rfmh.org (J.J. Foxe).

Available online on ScienceDirect (www.sciencedirect.com).

although neither study was designed to expressly investigate these processes.

Closure processes have been mostly studied using electrophysiological techniques. In a series of studies from this laboratory (Doniger et al., 2000; Foxe et al., 2001; Doniger et al., 2001a, 2002), line drawings of common objects, which were systematically fragmented to varying degrees, were used to study the timing of the neural processes responsible for perceptual closure. Our paradigm involved the presentation of sequences of fragmented pictures, whereby we began at very high levels of fragmentation and then incrementally increased the amount of information present in a given image until just enough of the object was present for subjects to “close” the picture (Snodgrass and Corwin, 1988; Doniger et al., 2000). Our studies revealed a robust event-related potential component termed the N_{CL} (for negativity associated with closure) that tracked the neural processes related to perceptual closure. This component was manifest as a relative negativity over bilateral occipito-temporal scalp and occurred in the 230–400 ms timeframe (Doniger et al., 2000), typically peaking at 290–300 ms. The scalp topography of this component suggested that it largely reflected neural activity from the LOC or nearby structures. In addition, based on our previous studies (Doniger et al., 2001a), we also hypothesized the existence of other generators outside the LOC (e.g., frontal regions) involved in closure. While topographic mapping has suggested the involvement of LOC regions in the generation of the N_{CL} , this has not been directly assessed. In the present study, we employed an integrative neuroimaging approach, combining the spatial accuracy of fMRI with the temporal resolution that ERP offers, to study the spatiotemporal dynamics of closure processes. We conducted a modified version of the perceptual closure experiment used in our previous work, while collecting both imaging and electrophysiological measures on the same subjects. This allowed us to co-register hemodynamic responses with electrical dynamics through the application of source analysis methods (Scherg and Picton, 1991; Grave de Peralta et al., 2001). Our data show that the bulk of N_{CL} activity is indeed generated within regions of the LOC. Furthermore, the timing of these processes, which can be derived from the electrical recordings, challenges models of perceptual closure that posit simple feed-forward mechanisms. Rather, our data suggest that closure processes occur relatively late in processing and are likely due to recursive processing within these structures, subsequent to an initial relatively automatic phase of object processing. Furthermore, through the application of source analysis, we were able to elucidate the time course of activity within the various generators involved in closure, allowing us to speak to temporal inter-relationships between these nodes of the object recognition circuit.

Materials and methods

Participants

Seven (4 female) neurologically normal paid volunteers, aged 21–35 (mean = 26), participated in the ERP study. Of these, six also participated in the fMRI section of the study in a counter-balanced order. Due to a mild bout of claustrophobia in the scanner, one of the seven ERP subjects had to be excluded from this portion of the study. All subjects provided written informed consent, and the procedures were approved by the Institutional

Review Board of the Nathan Kline Institute. All subjects reported normal or corrected-to-normal vision. All were right-handed.

Stimuli

Participants were presented with line drawings (black on a gray background) of natural and man-made objects. These were taken from sets of normed line drawings (Snodgrass and Vanderwart, 1980; Cywowitz et al., 1997). Images were 256×256 pixel bitmaps, divided into 16×16 segments. Segments containing black pixels were randomly and cumulatively deleted to produce seven incrementally fragmented versions of each picture (Snodgrass and Corwin, 1988). Level 1 refers to the complete picture and Level 8 to the most fragmented version, where the proportion of deleted segments for any level equals $[1 - 0.7^{(\text{level}-1)}]$. From these images, only pictures belonging to level three of fragmentation were utilized, hereafter simply referred to as “unscrambled pictures” (see Fig. 1A). Previous studies have shown that at this level of fragmentation subjects are most likely to identify the object, with the probability of the objects identified at this level being 0.73; nevertheless, it is important to note that even in cases where the object is not identified subjects experience the objectness of the image and the N_{CL} is still generated (Doniger et al., 2000, 2001b). A control set of scrambled pictures was generated by subjecting the unscrambled pictures to a randomization algorithm which randomly distributed the 16×16 segments such that they were structurally implausible and were not recognizable as objects (see Fig. 1A). The use of one stimulus level for the unscrambled pictures was motivated by the desire to design a relatively short experiment that would enable us to observe the closure effect (N_{CL}) without conducting the full ascending method of limits procedure of the previous studies which is highly time-consuming and hence not feasible for implementation in the MRI environment or in clinical settings.

Stimulus presentation

For the ERP section of the experiment, the stimuli were presented on a computer monitor (Iiyama Vision Master Pro 502, model # A102GT) located 143 cm from the subject. Images subtended an average of 4.8° ($\pm 1.4^\circ$) of visual angle in the vertical plane and 4.4° ($\pm 1.2^\circ$) in the horizontal plane. For the fMRI section of the study, the stimuli were delivered through MR-compatible liquid crystal display goggles (Resonance Technology Inc., Northridge, CA).

Timing of stimulus presentation

Timing of stimulus presentation for the fMRI study

The timing of presentations (Fig. 1B) for the fMRI section of the study was such that each image appeared for 750 ms followed by a blank screen for 2000 ms. Then, a “Y|N” response prompt appeared for 200 ms followed by a blank screen. Intertrial intervals were 2000–16,000 ms (see Fig. 1B). The scrambled and unscrambled stimulus conditions were randomly intermixed, resulting in an event-related design. A total of 160 unique images, 80 incomplete and 80 scrambled, were presented, and none was ever repeated. The stimuli were divided into five runs with equal distribution within each run. Division of the stimuli into five runs was done to provide breaks for the subjects. The duration of each run was approximately 7.5 min.

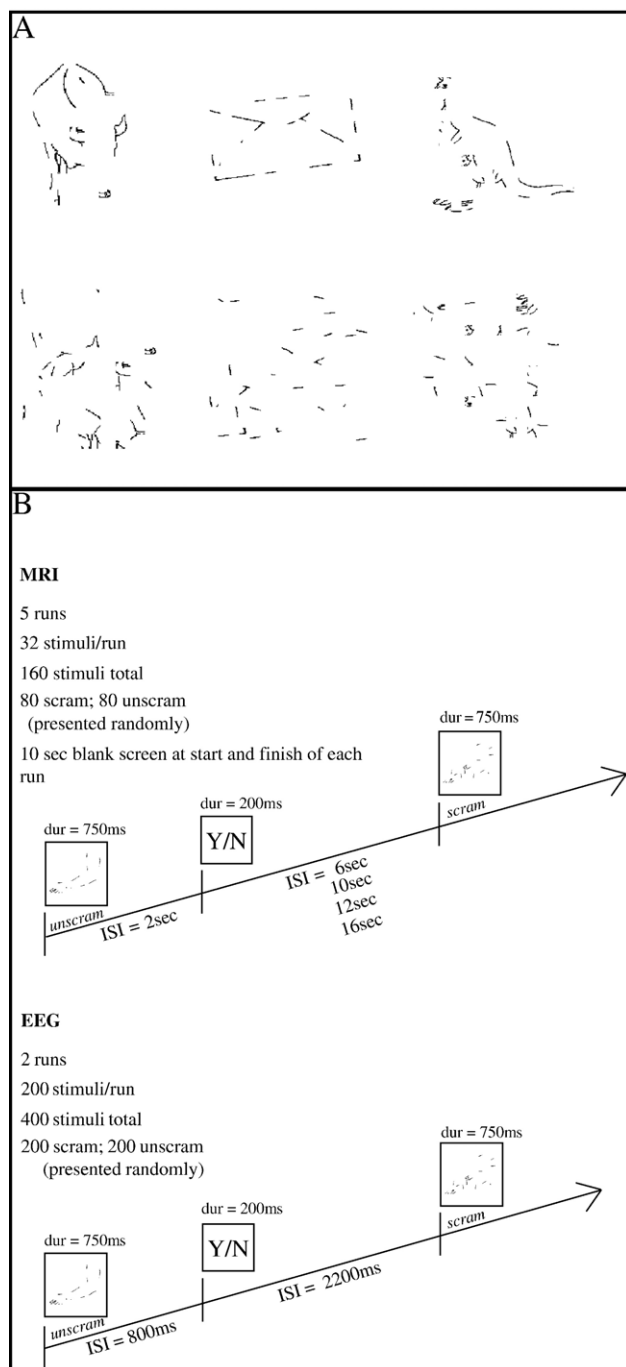


Fig. 1. (A) Examples of the stimuli: unscrambled (incomplete) line drawings are shown in the top panel, and scrambled line drawings are shown in the bottom panel. The figures from left to right are: bull, envelope, and kangaroo. (B) Schematic of the experimental paradigm, as implemented for fMRI (top) and EEG (bottom) recordings.

Timing of stimulus presentation for the ERP study

For the ERP section of the study, the timing of presentations (Fig. 1B) was such that each image appeared for 750 ms followed by a blank screen for 800 ms. Then, a “Y|N” response prompt appeared for 200 ms followed by a blank screen for 2200 ms. Subjects’ response window extended for 2300 ms from the onset of the “Y|N” prompt. Use of the response prompt was motivated by the desire to diminish the impact of motor responses on the sensory

ERP to the pictures. A total of 400 unique images, 200 incomplete and 200 scrambled, were presented in two runs, and no image was ever repeated. The images were randomly distributed with equal distribution in each run. The duration of each run was approximately 13 min.

Task

Subjects were instructed to press one button when they recognized the image as an object and another when they did not, following presentation of the “Y|N” prompt.

Measurements and analysis

fMRI data acquisition

A 3 T SMIS (Marconi) system equipped with a head volume coil at the Center for Advanced Brain Imaging (CABI) at the Nathan Kline Institute was used to acquire T2*-weighted echoplanar functional images (EPis) (TR = 2000, FA = 90, matrix size = 64×64 , FOV = 224 mm, voxel size = 3.5 mm^3) emphasizing the blood oxygenation level dependent (BOLD) response. In each run, 230 volumes (20 contiguous functional slices) were localized in an oblique-coronal orientation that covered the occipital lobes, as well as the posterior portions of the parietal and temporal lobes. High-resolution (1 mm^3) T1-weighted anatomical images of the whole brain were acquired from each subject using a standard three-dimensional magnetization prepared rapid gradient echo (MPRAGE) pulse sequence in order to allow volume statistical analyses of signal changes. Head movement was minimized with the use of a custom-made head holder. In all subjects, motion never exceeded 0.75 mm along any axis.

EEG data acquisition

Continuous EEG was acquired through Neuroscan Synamps using 128 scalp electrodes, impedances $<5 \text{ k}\Omega$, referenced to the nose, bandpass filtered from 0.05 to 100 Hz, and digitized at 500 Hz. For each subject, epochs extending from -100 ms prestimulus to 500 ms poststimulus were generated from the continuous EEG. These were averaged separately for both unscrambled and scrambled stimulus conditions to compute the VEP. Baseline was defined as -100 ms to stimulus onset. Trials with blinks and eye movements were rejected off-line on the basis of horizontal and vertical electro-oculograms (HEOG and VEOG). No systematic differences in HEOG and VEOG were observed across conditions. An artifact criterion of $\pm 60 \mu\text{V}$ was used at all other scalp sites to reject trials with excessive EMG or other noise transients. The average EEG epoch acceptance rate was 95%.

Data analysis

fMRI data analysis

The BrainVoyager 4.9 software package (Goebel et al., 1998) was used to analyze all fMRI data. Each subject’s data were analyzed separately. Preprocessing of functional scans was performed which included corrections for head movement, removal of linear trends, and high frequency temporal filtering. For each subject, their functional data were coregistered with their anatomical data. The functional data were then transformed into

Talairach space (Talairach and Tournoux, 1988) for the multi-subject analysis. To estimate the BOLD response associated with each condition, regressors representing the timing of each of the stimulation epochs were convolved with a canonical hemodynamic response function (Boynton et al., 1996) and used in a multiple regression analysis. The resulting statistical maps were then grouped to obtain activation maps. The P values of the statistical maps were corrected for multiple comparisons and z -normalized. Unscrambled and scrambled conditions were then contrasted using a general linear model (Friston et al., 1990, 1995). To observe the cortical activation, three-dimensional volume maps of the BOLD signal were created. For the purpose of presentation, the three-dimensional volume maps were loaded onto the Talairach-transformed brain of one subject.

Event-related potentials data analysis

Previous electrophysiological studies of closure processes (Doniger et al., 2000, 2001a) have measured and characterized the event-related potential component termed the N_{CL} which has been shown to be a robust measure of closure processes. The first phase of our analysis is based on these previous studies. We predefine the spatiotemporal dynamics of the closure process as characterized by N_{CL} . We therefore tested for the presence of N_{CL} over the lateral–occipital scalp regions by examining differences in the mean amplitude of the response between the unscrambled and scrambled responses by performing a 3-way repeated measure analysis of variance (ANOVA) with factors of stimulus (2: unscrambled and scrambled), hemispheres (2), and electrode (3 lateral–occipital sites).

A latency window of ± 20 ms was delineated around the peak of the N_{CL} (320 ms), and a measure of mean amplitude was derived. An alpha level of less than 0.05 was used for the statistical tests. The topographic distribution of the N_{CL} was also inspected in the difference voltage map. The initial topographic mapping was done using the “traditional” method of voltage mapping. These maps represent interpolated potential distributions, derived from the 128-scalp measurements and based on the computation of a common average reference. In addition, scalp current density (SCD) Laplacian topographic maps were calculated for spherical spline interpolated surface data (Perrin et al., 1987). The SCD map represents the second spatial derivative of the field potential and has the advantage of eliminating the effects of reference electrode and of reducing the volume conduction on the surface potential caused by tangential current flow within the scalp. Hence, the SCD map provides approximate locations of intracranial generators since it is less sensitive to contributions from more remote intracranial sources (Urbano et al., 1996).

The onset of the N_{CL} was determined using paired two-tailed t tests between the unscrambled and scrambled ERPs from electrode sites over occipito-temporal scalp regions, for the time window of 0–320 ms (where N_{CL} peaked). N_{CL} onset was defined as the point where the t test exceeded the 0.05 α criterion for at least 11 consecutive data points (>20 ms at 500 Hz digitization rate) (e.g., Guthrie and Buchwald, 1991; Murray et al., 2001).

In a previous electrophysiological study of closure processes (Doniger et al., 2001a), a negative going response for unscrambled compared to scrambled images over bilateral lateral–frontal regions was demonstrated. We therefore tested for the presence of this frontal effect on data within the timeframe of the N_{CL} (220–400 ms) from electrode sites over the bilateral lateral–frontal scalp region. To this end, a 3-way ANOVA with factors of stimulus (2:

unscrambled and scrambled), hemispheres (2), and electrode (3 frontal sites) was conducted.

As in the case of N_{CL} , the onset of the frontal effect was also determined using paired two-tailed t tests between the ERP responses to the unscrambled and scrambled images from electrode sites over the lateral–frontal scalp regions.

Source analysis and coregistration with fMRI data

A source model of the distributed network of activated brain regions was generated, and the fMRI data were used to cross-validate the modeled posterior sources. The coregistration of electrophysiological data (ERP) and hemodynamic data (fMRI-BOLD) from the same subjects (so-called multi-modal imaging) has been widely acclaimed as a major advance in our abilities to detail the spatiotemporal dynamics of brain function (e.g., Simpson et al., 1995; Martinez et al., 1999). However, coregistration of these separate data sets is based on the premise that the same neural events are represented in both, and it is therefore critical to consider the relationship or coupling between the physiological phenomena underlying the different signal modalities. Work by Logothetis and colleagues suggests that this is not an unreasonable premise. Intracranial electrophysiological recordings were compared to fMRI data concurrently recorded from the same monkeys (Logothetis et al., 2001), and it was found that the local field potential (i.e. the intracranial ERP) was strongly correlated with the BOLD response. They interpreted their data as strong evidence that both were indexing the same physiological events in the brain. The reader is referred to Murray et al. (2002) for a fuller exposition.

N_{CL} source localization

To estimate the neural generators underlying the N_{CL} , two methods of source localization were applied to data from the 280–340 ms time window of the grand average difference wave, where N_{CL} activity was observed to be greatest. These were brain electric source analysis (BESA) and local auto-regressive average (LAURA), described below. The resultant sources were compared and coregistered with the fMRI closure-related activations. We reasoned that similar sources across the different methodologies and approaches to source analysis would provide strong cross-validation of the findings.

Brain electric source analysis (BESA)

The basic premise of source modeling is that an observable deflection in the recording is related to a change in the local activity of a particular brain region. Therefore, a component can be defined as the part of the scalp waveform that results from the compound local activity of a circumscribed brain region (Scherg and von Cramon, 1985). BESA employs a least squares fitting algorithm, over which the user has interactive control. Source localization proceeds by a search within the head model for a location where the sources can explain a maximal amount of variance (Scherg and Picton, 1991). Here, we assumed bilateral symmetrical sources. An assumption of spatial symmetry considerably reduces the number of independent parameters to be determined (Scherg and Picton, 1991). We initially proceeded by using regional sources (Scherg and Picton, 1991). Each regional source is composed of three orthogonally co-localized dipoles that can have different orientations. This is advantageous when the neural generators from a given region are situated on different aspects of a gyral surface or sulcus such that they produce dipoles

from the same location but with different orientations. We later modeled the data by using a single dipole for a given location; this approach replicated the source localizations obtained by using regional sources. It is important to note that, in dipole source analysis, the modeled dipoles represent an oversimplification of the activity in the areas and should be considered as representative of centers of gravity of the observed activity rather than pinpoint localizations of exact generators (Murray et al., 2002; Dias et al., 2003; Molholm et al., 2004).

The LOC dipole sources were evaluated using the multiple source probe scan (MSPS) procedure as implemented in BESA 5.1. This function is based on the premise that, if the recorded EEG data have been adequately modeled, then an additional probe source would only show noise activity. In this procedure, the brain is scanned with a regional probe added to the existing solution. The power P of the probe source at location r in the signal interval is then compared with the power of the probe source in a reference interval:

$$q(r) = \sqrt{\frac{P(r)}{P_{\text{ref}}(r)}} - 1 \quad (1)$$

In the time-domain, the $q(r)$ is calculated using the source waveform of the probe source.

$P(r)$ is the mean power of the probe source at location r in the defined latency.

$P_{\text{ref}}(r)$ is the mean power of the probe source in the reference interval.

The inverse operator that estimates the power of the probe source uses a regularization constant of 4% for the modeled sources and a regularization constant of 0% by default.

The result of the MSPS for a good model yields an image indicating that the probe source has revealed activity around the locations of the modeled sources.

Local auto-regressive average (LAURA)

In a second independent source analysis, we estimated the sources in the brain using a distributed linear inverse solution based on a local auto-regressive average (LAURA) model of the unknown current density in the brain (Grave de Peralta et al., 2001). LAURA uses a realistic head model with a solution space of 4024 nodes, selected from a $6 \times 6 \times 6$ mm grid equally distributed within the gray matter of the Montreal Neurological Institute’s (MNI’s) average brain. Like other inverse solutions of this family, LAURA is capable of dealing with multiple simultaneously active sources of a priori unknown location and makes no assumptions regarding the number or location of active sources. This linearly distributed inverse solution selects the source configuration that best mimics the biophysical behavior of electric vector fields and produces a unique estimator of the current source density vector inside the brain. That is, the estimated activity at one point depends on the activity at neighboring points as described by electromagnetic laws (Grave de Peralta et al., 2001). This approach has been recently used in demonstrating the time course of the activity of intracranial generators for various cognitive tasks (Murray et al., 2005; Michel et al., 2001).

Whole epoch source modeling

In addition to modeling the neural generators underlying the N_{CL} (in the difference wave), we modeled the “unscrambled” response from 0 to 220 ms, the point at which the unscrambled and

scrambled responses first began to differ significantly, to obtain a model of the basic visual processing dynamics that preceded the N_{CL} . This analysis step allowed us to frame N_{CL} activations in the context of prior, presumably more elementary, visual processing activity.

Sources were modeled using the BESA software. A data-driven step-wise approach was employed, with each segment of the epoch that encompassed an ERP deflection successively fitted with a pair of symmetric sources. This resulted in three pairs of symmetrical dipoles modeling the positive deflection of the P1 (90–110 ms), the negative deflection of the N1 (140–180 ms), and the following positive deflection preceding the N_{CL} (the P2 from 200 to 220 ms). The resultant source waveforms were plotted to observe the time course of activation of each source across the 0 to 220 ms epoch and hence estimate the relative contributions of the different sources to a given scalp recorded deflection.

Results

fMRI results

The P values of the statistical maps obtained for each condition were Bonferroni corrected for multiple comparisons. Effects were accepted as significant only when P (corrected) < 0.001 . Both experimental conditions (unscrambled and scrambled) activated widespread and substantially overlapping cortical networks. To characterize the cortical activation associated with closure, we contrasted the relative activation to “unscrambled” pictures versus “scrambled” pictures. This revealed significantly greater activation ($P < 0.05$) in the unscrambled condition in bilateral regions corresponding to the LOC (Malach et al., 1995; Lerner et al., 2001). In addition to greater activation in the LOC bilaterally, there was greater activation of the temporo-parieto-occipital region (TPO) at the junction of areas 19 and 39 (see Table 1 and Fig. 2).

To understand the more dynamic aspects of the processes involved in closure, we then looked at the electrophysiological data.

Electrophysiological results

Inspection of group-averaged responses to each of the unscrambled and scrambled stimuli revealed the classic VEP

Table 1
fMRI clusters

Clusters	Talairach coordinates of the center of gravity of the cluster			P	t
	X	Y	Z		
Right lateral-occipital complex	34	−45	−15	0.03	2.178
Left lateral-occipital complex	−56	−50	−15	0.001	2.588
Right TPO (Fig. 2)	48	−53	24	0.04	1.979
Left TPO 1 (Fig. 2)	−29	−52	33	0.03	2.137
Left TPO 2 (Fig. 2)	−28	−62	50	0.001	2.587

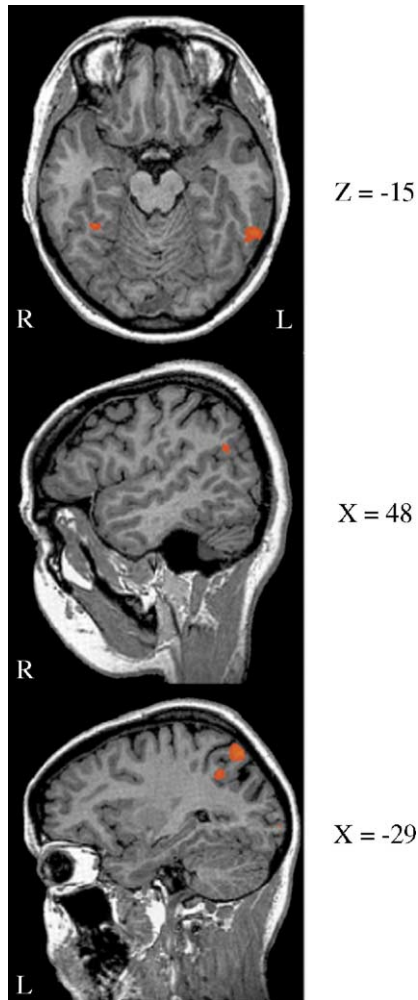


Fig. 2. fMRI results for the unscrambled versus scrambled comparison. The functional data are presented on the Talairach normalized brain of a single subject. All data are $P \leq 0.05$, corrected for multiple comparisons across the entire image volume. Top: axial view showing areas of significant BOLD signal increase in the ventral stream regions of LOC. Middle: sagittal view showing significant BOLD signal increase in right TPO. Bottom: sagittal view showing significant BOLD signal increase in the left TPO inferiorly and left parietal area superiorly.

componentry, with the P1 peaking at 88 ms, the N1 at 160 ms, and the P2 at 220 ms. These components were maximal over posterior scalp sites and, as in our previous studies, did not differ between the unscrambled and scrambled conditions.

Lateral–occipital N_{CL} activity

As expected, over the ~ 220 –400 ms time window, the unscrambled response was negative going with respect to the scrambled response, with the difference peaking at 320 ms. This relative negative deflection has been shown to track perceptual closure and has been termed the N_{CL} for negativity associated with closure (Doniger et al., 2000). The SCD map at the peak of the difference (for the unscrambled minus scrambled difference waveform) showed a bilateral occipito-temporal distribution that extended somewhat dorsally to temporo-parietal regions (Fig. 3).

This difference was tested with a repeated measure ANOVA (condition (2: unscrambled and scrambled) by hemisphere (2) by electrode (3 each over right and left lateral–occipital scalp: PO5/

PO6, PO7/PO6, P3/PO4)) on the mean amplitude data from a 40 ms window centered at the peak of the N_{CL} as determined in the grand mean waveform ($320 \text{ ms} \pm 20 \text{ ms}$). A significant main effect of condition ($F(1,6) = 26.9, P < 0.002$) confirmed the presence of the N_{CL} . No significant interaction between condition and hemisphere or electrode was found. The running t tests on data from lateral–occipital sites revealed that the N_{CL} onset at 218 ms over the left hemisphere and 224 ms over the right.

Frontal closure-related activity

Our data also showed a negative going response to unscrambled compared to scrambled images over bilateral lateral–frontal regions (see Fig. 3). An ANOVA was performed on data from the timeframe of the N_{CL} (270–400 ms), from electrode sites over the bilateral fronto-temporal scalp (conditions (2: unscrambled and scrambled) \times 2 hemispheres \times electrodes (3 frontal electrodes: F5/F6, FC5/FC6, FT7/FT8)). There was a significant main effect of condition ($F(1,6) = 29.25, P < 0.002$), with no interaction between condition and hemisphere or electrode. To place the onset of the fronto-temporal activity with respect to the onset of the posterior N_{CL} activity, running t tests were performed on three representative pairs of frontal electrode sites (F5/F6, FC5/FC6, FT7/FT8). This analysis indicated that the onset of the significant frontal activity was 270 ms over the left hemisphere and 272 ms over the right, peaking at about 370 ms, and was sustained throughout the remaining epoch. This onset was about 50 ms after the onset of N_{CL} and about 50 ms before the peak amplitude of the N_{CL} .

Dipole source analysis

N_{CL} source localization. A major emphasis of this study was the localization of the intracranial generators of N_{CL} . Source modeling of the N_{CL} with BESA resulted in dipoles situated bilaterally in lateral–occipital regions.

The model produced a goodness-of-fit value of 95.00% (residual variance = 5.00%) across the modeled epoch (280–340 ms). These bilateral dipoles showed a remarkably close correspondence to the fMRI activations found for the same subjects in LOC (see Fig. 4A). After fixing the location and orientation of these dipoles, an additional pair of symmetrical dipoles was seeded in dorsal visual regions based on the dorsally located fMRI activations, with their orientation allowed to freely fit. The addition of these dipoles only accounted for an additional 1.2% of the explained variance, suggesting that, in this time, range dorsal contributions to the N_{CL} were relatively weak at best. The addition of a test dipole to the original two-dipole solution did not affect their activity, suggesting an optimal solution across the epoch (Scherg and Picton, 1991).

The results obtained using the local auto-regressive approach (LAURA) similarly indicated the presence of sources in the lateral–occipital regions in the 280–340 ms epoch, which extended from LOC to slightly more dorsal regions of occipital cortex (Fig. 5). Thus, LAURA, BESA, and fMRI data all converge on the finding of N_{CL} generators situated substantially within the LOC. It should be pointed out that both source localization techniques, while highly consistent in pointing to the LOC as the major or central generator complex of the N_{CL} , do not possess the spatial resolution necessary to rule out contributions from neighboring regions such as V4 that may also contribute in part to the N_{CL} signal. Furthermore, since we did not use retinotopic mapping procedures here to delimit the borders of the earlier

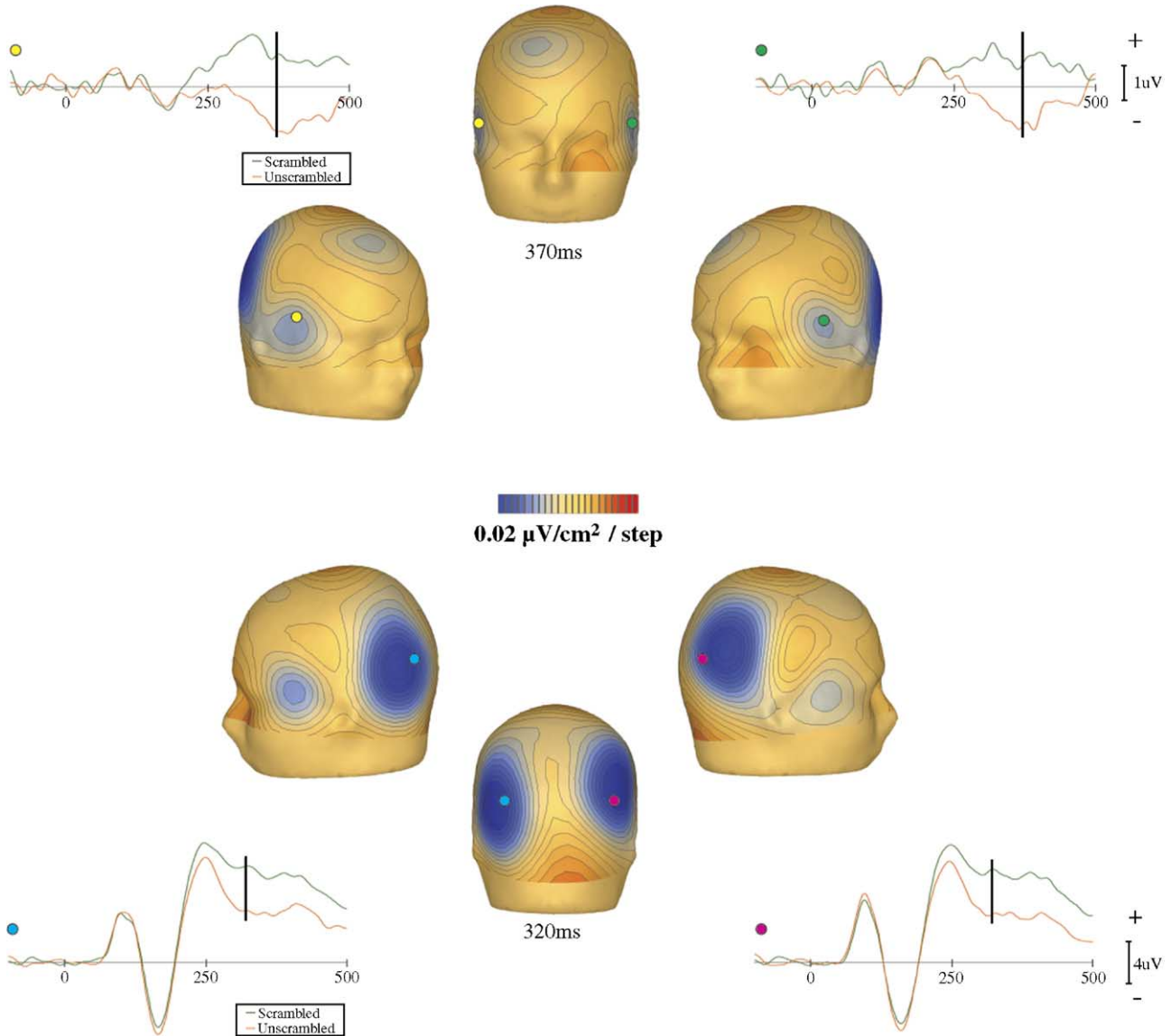


Fig. 3. ERP responses to the unscrambled and scrambled stimuli over frontal and posterior scalp and scalp current density (SCD) maps of the difference. Top: SCD maps at 370 ms showing the observed negativity focused over fronto-temporal scalp. The graphs show scalp recordings from two representative frontal electrodes (F5/F6). The unscrambled stimulus condition (in red) produced larger negativity when compared to the scrambled pictures (in green). The point of maximal difference is indicated with a black bar. Bottom: SCD maps at 320 ms (peak N_{CL} activity) illustrate the relative negativity over lateral-occipital scalp for unscrambled versus scrambled stimuli. The graphs show scalp recording from 2 representative electrodes PO6/PO7. The unscrambled stimulus condition (in red) produced larger negativity when compared to the scrambled pictures (in green). The point of maximal difference is indicated with a black bar.

sensory regions during fMRI measures (e.g., Warnking et al., 2002; Slotnick and Yantis, 2003), it is similarly possible that the activation clusters found here extend back into hierarchically earlier cortices. As such, the present results simply point to a predominant contribution from LOC regions but do not rule out additional neighboring sources.

Whole epoch source modeling. To place the N_{CL} activations within the context of the basic visual processing dynamics that preceded the N_{CL} , we modeled the intracranial sources for this time period (0 to 220 ms) for the response to the unscrambled pictures.

This was done by fitting dipoles to the three major deflections in a step-wise fashion. The first pair of symmetrical dipoles was fit to the P1 (90–110 ms) and achieved a best-fit in dorsal regions of

the occipital cortices; a pair of dipoles subsequently fit within the latency range of the N1 (140–180 ms) achieved a best-fit within the TPO cortical region (see green and dark pink dipoles in Figs. 4 and 6); and a final symmetrical pair fitted to the positive deflection preceding the N_{CL} (“P2”, 200–220 ms) resulted in a best-fit in the region of the LOC, closely corresponding to those in the source model of the N_{CL} (Figs. 4 and 6). These three pairs of symmetrical dipoles produced an optimal model for the epoch, with a goodness-of-fit value of 93% (residual value = 7%). Fig. 6 shows the dipole sources with the corresponding source waveforms, and Fig. 4B shows the correspondence of the fMRI activations with the dipole sources.

The source waveforms show dorsal and ventral contributions to the pre- N_{CL} epoch components, consistent with previous reports

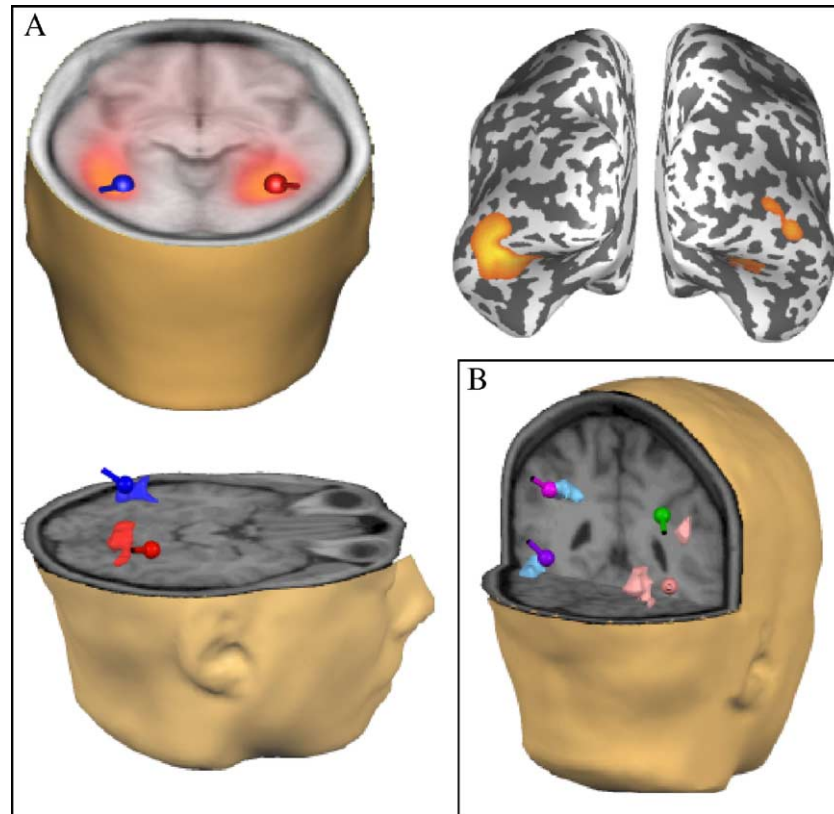


Fig. 4. (A) Dipole solution for source localization of the N_{CL} . Top left: N_{CL} dipolar sources are localized to the LOC. These dipoles were obtained by fitting the difference waveform over the 280–340 ms period and resulted in a goodness-of-fit value of 95%. This figure also shows the MSPS image over the same period (orange shading). Top right: the computed MSPS image is projected onto a Talairach-transformed inflated brain (occipital view). Bottom left: the same dipoles are coregistered with the fMRI data from the unscrambled versus scrambled contrast. This illustrates the close correspondence of the independently derived N_{CL} localizations from ERP and fMRI recordings. (B) This 3D reconstruction of fMRI activations for the unscrambled versus scrambled conditions illustrates the significantly greater activity for the unscrambled condition in bilateral LOC and TPO (the right hemisphere in pink and the left in blue). These activations are coregistered with the independently derived dipole source solutions (from the ERP response to the unscrambled stimuli). The location of the dipoles fitted over the time course of the N1 shows a close correspondence with the fMRI activations in the TPO; and the location of the dipoles fitted to the P2 just prior to the onset of the N_{CL} shows a close correspondence with the fMRI activations in the LOC.

(Di Russo et al., 2001). The dorsal sources in the occipital cortices contributed to all three components, whereas the sources in the temporo-parietal region contributed only to the earlier components, the P1 and N1. This modeling of the pre- N_{CL} activity shows that LOC contributes to the early visual componentry as well as to the later N_{CL} . This is consistent with a model of object recognition in which successively more complex object information is extracted through recursive processing in the general cortical region of the LOC (see Doniger et al., 2001a,b).

Discussion

The high spatial resolution of fMRI was married with the millisecond temporal resolution of ERPs to assess the generators of perceptual closure processes, as indexed by the N_{CL} component of the visual evoked potential. A major role for regions of bilateral LOC and frontal cortex in these processes was confirmed, and a concomitant role for dorsal visual regions was suggested. Here, we discuss the spatiotemporal dynamics of these object recognition processes in the context of the timing and regional distribution of ongoing visual sensory processing. Our results suggest that there are multiple phases of processing within the LOC and that closure

processes are delayed until a relatively late phase of processing within this complex.

Multiple phases of processing within LOC

Source analysis of early visual processing during the sensory processing stages preceding the N_{CL} revealed the expected activations of both dorsal and ventral regions of visual cortex, consistent with previous source modeling studies (e.g., Di Russo et al., 2001; Simpson et al., 1995). Ventral activity localized to the LOC was seen to begin well before 100 ms (i.e., during the timeframe of the P1 component) and to continue through the time course of the N1 component and finally the N_{CL} . That is, there were multiple phases of processing within LOC and neighboring regions, but only processing over the later phase during the N_{CL} was modulated due to “closure”.

Previous data from both human and monkey electrophysiological studies are consistent with this notion of recurrent rounds of processing within LOC (see Foxe et al., 2005). Monkey infero-temporal (IT) cortex appears to be the functional homologue of human LOC as these regions share great similarities in their response properties. For example, both IT neurons (Sary et al., 1993) and LOC (Grill-Spector et al., 1998) show cue-invariant

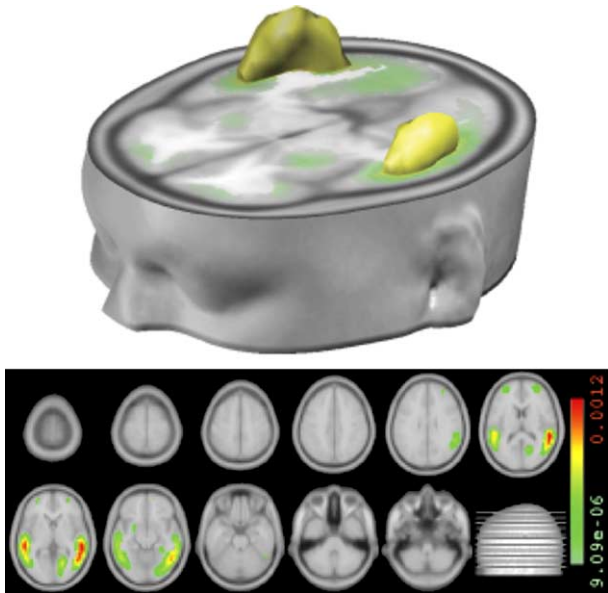


Fig. 5. 3D reconstruction of the inverse solution obtained using LAURA (top). In the lower half of the figure, the LAURA solution is superimposed on MRI slices of a Montreal brain, showing significant ($P < 0.01$) activation that is greatest in the LOC.

object recognition, whereby the neural representation of a given visual object remains constant regardless of the cues used to define that object (e.g., luminance, texture, or motion). The relatively early initial activation of LOC (~80 ms) is consistent with monkey data showing the activation in IT onsets by 40–50 ms (e.g.,

Schroeder et al., 1998, 2001). High-density scalp topographic mapping in humans has also shown activation of the LOC region of the ventral visual stream by as little as 70–80 ms (Foxe and Simpson, 2002), consistent with the present findings. Indeed, LOC has been shown to be involved in object recognition processes for illusory contour stimuli beginning as early as 90–100 ms (e.g., Murray et al., 2002, 2004; Foxe et al., 2005). Furthermore, a number of studies have implicated the N1, with a peak latency falling between 140 and 180 ms and underlying neural generators in the LOC (Di Russo et al., 2001), in the structural encoding of object information (Bentin and Golland, 2002; Doniger et al., 2001a; Eimer, 2000; Rossion et al., 2000). Collectively, these studies show that several iterations of processing occur in LOC prior to object recognition. It should be noted though that LOC likely comprises a number of functional subdivisions and that these smaller regions may be differentially engaged in the various phases of processing over time. The spatial resolution of source modeling is presently too crude to allow for a more detailed delineation of this possibility, and the lack of temporal information inherent in fMRI also precludes any teasing apart of these phases.

Perceptual versus conceptual processing within LOC

Turning again to the issue of multiple rounds of processing within LOC, the question becomes what the nature of the processing that each of these phases represents. When objects are clearly identifiable, previous studies from our laboratory have found that object recognition effects are typically seen much earlier, during the N1 component, which is also clearly generated within the same LOC structures as the N_{CL} (e.g., Murray et al., 2002, 2004). Thorpe and his group have also shown that

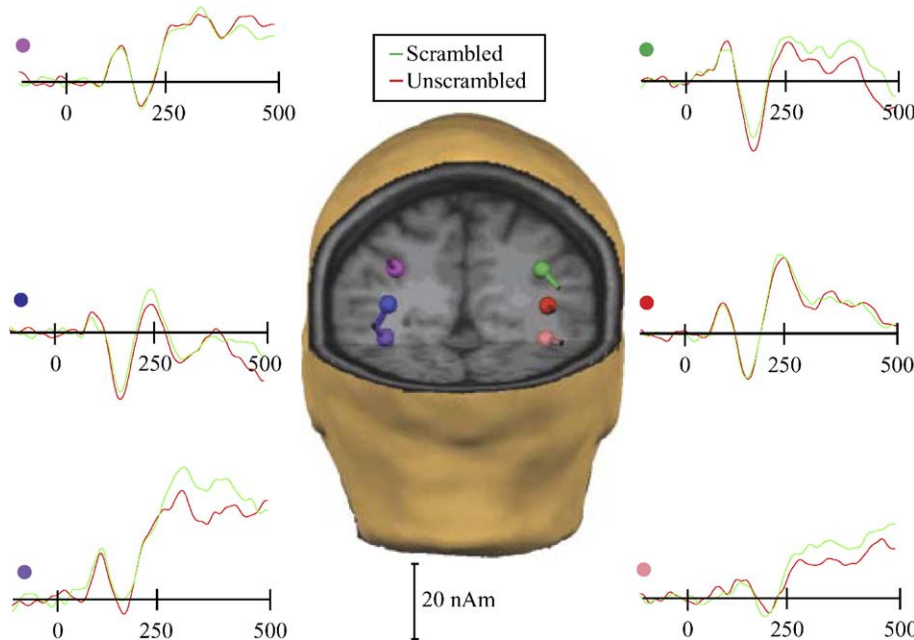


Fig. 6. The dipolar solution obtained for step-wise modeling of the major deflections in the ERP response to the unscrambled stimuli (i.e., the P1, N1, and the P2 prior to N_{CL} activity). Dipoles are shown in the Talairach-transformed brain of an individual subject. The corresponding source waveforms illustrate the time course of these dipoles. Color dots by the source waveforms indicate the corresponding color-matched dipole. Fitting of the activity over the time course of the P1 component resulted in a pair of dipoles positioned within dorsal visual regions (see middle pair of dipoles in blue and red). Fitting of the activity over the time course of the N1 component resulted in a pair of dipoles situated in TPO (top pair of dipoles shown in dark pink and green). Fitting activity over the time course of the P2 just prior to the onset of the N_{CL} resulted in a pair of dipoles situated within the LOC (see lower pair of dipoles in purple and light pink).

differentiation of complete natural images occurs automatically during early processing stages (e.g., Thorpe et al., 1996; Rousselet et al., 2004). On the other hand, when objects are highly degraded and more effortful extraction of object information is necessary, processing moves to the later N_{CL} ¹, and we have found that the N_{CL} builds in amplitude across a series of pre-recognition levels. As such, we interpreted it as indexing neural processes responsible for the extraction of successively greater levels of object identity in line with models suggesting that the pre-recognition stages of object processing in LOC involve the extraction of successively more complex object primitives (Marr and Nishihara, 1978; Biederman, 1987; Malach et al., 1995). These findings have led us to propose a model of object processing whereby the initial LOC activity, especially in the timeframe of the N1, represents a relatively automatic “perceptual” level of object processing, and the subsequent N_{CL} represents an effortful “conceptual” level of processing within the same structures. We conceive of this second level of processing as being invoked when the initial automatic processing represented during the early processing phases (P1 and N1) fails to fully reveal a given object’s identity (Doniger et al., 2001a,b; see Tulving and Schacter, 1990 for a similar model).

A distributed network of regions interacts with LOC during “closure” processes

In our data, we see that the onset of N_{CL} activity is followed by fronto-temporal activity. This suggests to us that a good match between inputs and perceptual representation in the LOC results in the activation of the object’s corresponding semantic/episodic elements, most likely through connections between LOC and fronto-temporal regions. In non-human primate studies, frontal regions have been shown to trigger memory retrieval of visual object representations in IT, the functional homologue of LOC (Miyashita and Hayashi, 2000), and there are direct connections from IT and TE to prefrontal cortex (Cavada and Goldman-Rakic, 1989; Cavada et al., 2000; Rempel-Clower and Barbas, 2000); what is more, pathways connecting the dorsolateral prefrontal cortex with the hippocampal formation and parahippocampal cortex have also been shown and been associated with functions involving working memory and semantic information processing (Goldman-Rakic, 1992; Goldman-Rakic et al., 1984). The onset of fronto-temporal activity ~50 ms into closure processes (i.e., the N_{CL}) that we see here likely reflects the activation of this semantic/episodic information.

Dorsal contributions to object recognition processes

The model of the pre- N_{CL} epoch showed substantial dorsal contributions to all of the modeled components, the P1, N1, and the P2, the last of which just preceded N_{CL} onset. However, in this study, there is no significant difference between dorsal activations for the two stimulus types, which might be taken to suggest that dorsal structures do not play a central role in object processing or closure. However, we believe that dorsal processing is likely a necessary building block of normal object recognition.

In support of the role of early dorsal stream contributions to object recognition, recent studies in patients with schizophrenia are

potentially revealing. It has been shown that these patients exhibit severe deficits in early dorsal stream processing as represented by a large decrement in amplitude of the dorsal P1 component (e.g., Foxe et al., 2001; Doniger et al., 2002; Spencer et al., 2004; Foxe et al., 2005). Critically, these patients also fail to generate the N_{CL} component and are severely impaired in their abilities to perform perceptual closure (see Doniger et al., 2002). In other words, conceptual-level object processing is severely impaired. We proposed that it was the initial breakdown in dorsal stream processing that ultimately led to this late-phase object recognition deficit. We arrived at this hypothesis because it was also clear from our recordings that the intervening N1 component, during the putatively automatic phase of processing, was of normal latency and amplitude, strongly suggesting that ventral stream areas were not themselves directly impaired. A subsequent study established that ‘automatic’ object processing, indexed neurophysiologically by the N1, was indeed intact in this population (Foxe et al., 2005), again despite large-scale deficits in the preceding dorsal P1 component. Additional evidence that dorsal stream processing is important to object recognition comes from Murray et al. (2002), in which it was shown that P1 amplitude over dorsal visual structures was systematically related to the spatial extent or distribution of object parts. As such, we posited that one of the initial functions of the dorsal visual stream was to spatially delineate object features for subsequent analysis by the ventral stream (i.e. LOC). In the present study, however, the spatial extent of both scrambled and unscrambled pictures does not vary, so mechanisms for delineating spatial extent of object parts would not be expected to show any modulation. In summary, these results, taken together, suggest that early dorsal processing plays an important role in subsequent conceptual-level object processing. Crossover inputs from dorsal to ventral visual regions have been shown through intracranial recordings in awake-behaving macaques (e.g., Schroeder et al. 1998), demonstrating the feasibility of the dorsal stream feeding into ventral object recognition processes.

Frontal contributions to “closure”: Distinction between N_{CL} and N350

A frontally distributed component (N350) in response to recoverable versus irrecoverable pictures has been characterized (Schendan and Kutas, 2002). The investigators attributed this component to identification processes, and asserted that the N_{CL} was likely to be the same component as their frontal N350. However, the contention that the N_{CL} represents the same process as the frontal N350 in their recordings is not supported on a number of empirical counts. First, these authors posited that the lateral–occipital distribution of the N_{CL} , which we have repeatedly shown (Doniger et al., 2000, 2001a, 2002), was a reflection of our positioning of the reference electrode on the nose. This cannot be the case as the distributions shown in our previous work and again here are based on the Laplacian current-source density estimation, which is reference free. The present localization based on both ERP and fMRI evidence shows definitively that the major sources of the N_{CL} are in the LOC. Second, our previous work was quite clear in showing that, while N_{CL} was of greatest amplitude at the point of object identification, it was also modulated at levels of object fragmentation preceding explicit identification. As such, it was clearly related to object processing rather than identification itself, unlike the frontal N350. Furthermore, our previous work also showed that frontal regions were selectively activated at the point

¹ A similar delay in selective processing for objects is seen in monkey IT when objects are occluded (Kovacs et al., 1995).

of object identification itself but that this was an “all-or-none” process. That is, the frontal differentiation was not modulated over pre-recognition steps but only at recognition (see Doniger et al., 2002). Another important distinction between the N_{CL} and the frontal N350 described in the work of Shendan and Kutas is that the N_{CL} is greatest (most negative) at the level of identification, while their N350 is smaller for the identified objects when compared to unidentified objects. Here, we have defined the spatiotemporal dynamics of two distinct processes, namely the lateral–occipital N_{CL} negativity on the one hand and a fronto-temporal negativity on the other. In our conceptualization of these scalp negativities, the object completion process as indexed by the peak N_{CL} activity and object selection processes involving the frontal brain areas are not mutually exclusive but rather important functional steps involved in the process of object recognition. It should be pointed out here that, due to lack of coverage of the frontal areas during fMRI acquisition, all discussion of the involvement of frontal regions in closure processes is derived from the ERP data.

Two possible models of object recognition processes

A bottom–up hierarchical model

Some models of object completion, particularly in computational vision, are based on bottom–up processing (Zemel and Mozer, 2001; Vecera and Farah, 1997). In a bottom–up hierarchical model, it is thought that the visual information in a scene is first extracted in lower visual areas and then projected to higher-level areas that respond to increasing levels of complexity, until a visual representation of the object is formed. The data-driven representation is then associated with representations in memory to bring about object recognition. This model is attractive because increasing complexity is clearly a feature of neurons at each of the ascending levels of the visual hierarchy (e.g., V1 to V2 to V4 to IT). Area V1 contains columns of cells that show preference for simple basic features such as orientation (Hubel and Wiesel, 1962). Further along the visual pathway, area V4 responds well to features having a medium level of complexity (Pasupathy and Connor, 1999). Monkey IT (Sary et al., 1993) and human LO (Grill-Spector et al., 1998) show cue-invariant object recognition and belong to higher-level regions where a visual representation of the object image is formed (Tanaka, 1996). Anatomically, such a model takes into account the contributions of feed-forward connections while ignoring the role of the numerous parallel and feed-back connections (Bullier and Nowak, 1995). Functionally, a bottom–up model will allow only for a direct mapping of object primitives to object representations; on the other hand, if one takes into account the contributions of both the feed-forward and feed-back connections in a convergent model, then one would allow for the comparison of the input with the possible multiple object representations stored in memory (Bar, 2003).

A convergent model for closure processing

Many models have been proposed that take into account the contribution of feed-forward as well as feed-back connections (Kosslyn et al., 1995; Ullman, 1995; Viggiano and Kutas, 2000). In addition, a number of studies have indicated that feed-back processes play an important modulatory role in the time course of events (Bullier, 2001; Bullier et al., 2001; Engel et al., 2001; Lamme and Spekreijse, 2000). The time course of activities

observed in the source waveforms here of the generators in the dorsal and ventral visual streams reveals periods of simultaneous activity during object recognition processes. In addition, the onset of the activity in the frontal regions is ~ 50 ms before the peak of the N_{CL} . These patterns of activity seem to favor a model whereby converging streams of information from occipital and frontal regions are involved in closing the image.

Anatomical connections from V1 and V2 to V4 and IT have been shown (Nakamura et al., 1993). Additionally, direct connections between V4 and TE (Felleman and Van Essen, 1991), from IT to prefrontal cortex (Cavada and Goldman-Rakic, 1989; Cavada et al., 2000), and from TE to prefrontal cortex (Rempel-Clower and Barbas, 2000) have been demonstrated. Many of these connections are thought to originate from the magnocellular pathway (Barbas, 1995). The prefrontal cortex is thought to be involved in functions such as guessing, hypothesis generation (Petrides et al., 2002), and in the selection of currently relevant memories (Schnider et al., 2000). It has been suggested (Bar, 2003) that the magnocellular connections to the prefrontal cortex convey a course representation of the object to the prefrontal cortex where a set of predictions is made about the identity of the object. This new information, which could serve to limit the number of possible matches among the many alternatives from memory (Thompson-Schill et al., 1999), is then back-projected to aid the process of closure. Once closure is achieved, the new information is then re-projected to the prefrontal cortex for the purpose of retrieval of the semantic information (Wagner et al., 2001). The involvement of memory in closure processing is also supported by our recent finding that hippocampus is differentially activated during this process (Sehatpour et al., 2004).

While these data show that feed-back-recurrent processing is a critical component of closure processes for fragmented or impoverished stimuli, what we have termed the “conceptual” mode of processing, it might be argued that, when complete and unambiguous object information is presented, the system can rely entirely on feed-forward processing. By this conception, our original classification of the fast automatic “perceptual” mode of processing could be equated with a simple feed-forward model. While this may be an attractive distinction, data from monkey intracranial studies (Hupe et al., 1998, 2001; Bullier et al., 2001; Girard et al., 2001) have shown that feed-back processing is already a major contributor to ongoing stimulus analysis from the moment of initial afference in the primary visual cortex. As such, even automatic and simple object recognitions are likely to depend on feed-back processing. Considerable work remains to be done to determine the respective roles of feed-forward and feed-back processes in the various forms of object recognition.

Conclusion

High-density electrical mapping, source analysis, and functional neuroimaging were used to map the spatiotemporal dynamics of perceptual closure processes. The data strongly support a model in which object recognition is achieved through interplay between the LOC and frontal cortical regions. The current data, together with findings from previous studies, indicate that there are dorsal and ventral contributions to object recognition and that frontal regions are activated for explicit object recognition only once there is a good match between the input and a representation in the LOC.

Acknowledgments

This work was supported by grants from the National Institute of Mental Health (MH65350 to JJF and MH49334 to DCJ) and a grant from the National Institute on Aging (AG22696 to JJF). SM is supported by a Kirschstein National Research Service Award (NRSA) post-doctoral fellowship (MH068174). The authors would like to express their sincere appreciation to Dr. Vance Zemon for his insights. Deirdre Foxe and Beth Higgins provided invaluable technical help with data collection. We would also like to thank the team at the Cognitive Neurophysiology Laboratory (<http://cogneuro-nki.rfmh.org/>) without whose help this project could not have been completed.

References

- Bar, M., 2003. A cortical mechanism for triggering top-down facilitation in visual object recognition. *J. Cogn. Neurosci.* 15, 600–609.
- Barbas, H., 1995. Anatomic basis of cognitive–emotional interactions in the primate prefrontal cortex. *Neurosci. Biobehav. Rev.* 19, 499–510.
- Bartlett, F.C., 1916. An experimental study of some problems of perceiving and imagining. *Br. J. Psychol.* 8, 222–226.
- Bentin, S., Golland, Y., 2002. Meaningful processing of meaningless stimuli: the influence of perceptual experience on early visual processing of faces. *Cognition* 86, B1–B14.
- Biederman, I., 1987. Recognition-by-components: a theory of human image understanding. *Psychol. Rev.* 94, 115–147.
- Boynton, G.M., Engel, S.A., Glover, G.H., Heeger, D.J., 1996. Linear systems analysis of functional magnetic resonance imaging in human V1. *J. Neurosci.* 16, 4207–4241.
- Bullier, J., 2001. Integrated model of visual processing. *Brain Res. Brain Res. Rev.* 36, 96–107.
- Bullier, J., Nowak, L.G., 1995. Parallel versus serial processing: new vistas on the distributed organization of the visual system. *Curr. Opin. Neurobiol.* 5, 497–503.
- Bullier, J., Hupe, J.M., James, A.C., Girard, P., 2001. The role of feedback connections in shaping the responses of visual cortical neurons. *Prog. Brain Res.* 134, 193–204.
- Cavada, C., Goldman-Rakic, P.S., 1989. Posterior parietal cortex in rhesus monkey: II. Evidence for segregated corticocortical networks linking sensory and limbic areas with the frontal lobe. *J. Comp. Neurol.* 287, 422–445.
- Cavada, C., Company, T., Tejedor, J., Cruz-Rizzolo, R.J., Reinoso-Suarez, F., 2000. The anatomical connections of the macaque monkey orbitofrontal cortex. A review. *Cereb. Cortex* 10, 220–242.
- Cycowicz, Y.M., Friedman, D., Rothstein, M., Snodgrass, J.G., 1997. Picture naming by young children: norms for name agreement, familiarity, and visual complexity. *J. Exp. Child Psychol.* 65, 171–237.
- Denys, K., Vanduffel, W., Fize, D., Nelissen, K., Peuskens, H., Van, E.D., 2004. The processing of visual shape in the cerebral cortex of human and nonhuman primates: a functional magnetic resonance imaging study. *J. Neurosci.* 24, 2551–2565.
- Di Russo, F., Martinez, A., Sereno, M.I., Pitzalis, S., Hillyard, S.A., 2001. Cortical sources of the early components of the visual evoked potential. *Hum. Brain Mapp.* 15, 95–111.
- Dias, E.C., Foxe, J.J., Javitt, D.C., 2003. Changing plans: a high density electrical mapping study of cortical control. *Cereb. Cortex* 13, 701–715.
- Doniger, G.M., Foxe, J.J., Murray, M.M., Higgins, B.A., Snodgrass, J.G., Schroeder, C.E., 2000. Activation timecourse of ventral visual stream object-recognition areas: high density electrical mapping of perceptual closure processes. *J. Cogn. Neurosci.* 12, 615–621.
- Doniger, G.M., Foxe, J.J., Schroeder, C.E., Murray, M.M., Higgins, B.A., Javitt, D.C., 2001a. Visual perceptual learning in human object recognition areas: a repetition priming study using high-density electrical mapping. *NeuroImage* 13, 305–313.
- Doniger, G.M., Silipo, G., Rabinowicz, E.F., Snodgrass, J.G., Javitt, D.C., 2001b. Impaired sensory processing as a basis for object-recognition deficits in schizophrenia. *Am. J. Psychiatry* 158, 1818–1826.
- Doniger, G.M., Foxe, J.J., Murray, M.M., Higgins, B.A., Javitt, D.C., 2002. Impaired visual object recognition and dorsal/ventral stream interaction in schizophrenia. *Arch. Gen. Psychiatry* 59, 1011–1020.
- Eimer, M., 2000. The face-specific N170 component reflects late stages in the structural encoding of faces. *NeuroReport* 11, 2319–2324.
- Engel, A.K., Fries, P., Singer, W., 2001. Dynamic predictions: oscillations and synchrony in top-down processing. *Nat. Rev., Neurosci.* 2, 704–716.
- Felleman, D.J., Van Essen, E., 1991. Distributed hierarchical processing in the primate cerebral cortex. *Cereb. Cortex* 1, 1–47.
- Foley, M.A., Foley, H.J., Durso, F.T., Smith, N.K., 1997. Investigations of closure processes: what source-monitoring judgments suggest about what is “closing”. *Mem. Cogn.* 25, 140–155.
- Foxe, J.J., Simpson, G.V., 2002. Flow of activation from V1 to frontal cortex in humans. A framework for defining “early” visual processing. *Exp. Brain Res.* 142, 139–150.
- Foxe, J.J., Doniger, G.M., Javitt, D.C., 2001. Early visual processing deficits in schizophrenia: impaired P1 generation revealed by high-density electrical mapping. *NeuroReport* 12, 3815–3820.
- Foxe, J.J., Murray, M.M., Javitt, D.C., 2005. Filling-in in schizophrenia: a high-density electrical mapping and source-analysis investigation of illusory contour processing. *Cereb. Cortex*. doi:10.1093/cercor/bhi069.
- Friston, K.J., Frith, C.D., Liddle, P.F., Dolan, R.J., Lammertsma, A.A., Frackowiak, R.S., 1990. The relationship between global and local changes in PET scans. *J. Cereb. Blood Flow Metab.* 10, 458–466.
- Friston, K.J., Holmes, A.P., Worsley, K.J., Poline, J.P., Frith, C.D., Frackowiak, R.S.J., 1995. Statistical parametric maps in functional imaging: a general linear approach. *Hum. Brain Mapp.* 2, 189–210.
- Gerlach, C., Aaside, C.T., Humphreys, G.W., Gade, A., Paulson, O.B., Law, I., 2002. Brain activity related to integrative processes in visual object recognition: bottom-up integration and the modulatory influence of stored knowledge. *Neuropsychologia* 40, 1254–1267.
- Girard, P., Hupe, J.M., Bullier, J., 2001. Feedforward and feedback connections between areas V1 and V2 of the monkey have similar rapid conduction velocities. *J. Neurophysiol.* 85 (3), 1328–1331.
- Goebel, R., Linden, D.E., Lanfermann, H., Zanella, F.E., Singer, W., 1998. Functional imaging of mirror and inverse reading reveals separate coactivated networks for oculomotion and spatial transformations. *NeuroReport* 9, 713–719.
- Goldman-Rakic, P.S., 1992. Working memory and the mind. *Sci. Am.* 267, 110–117.
- Goldman-Rakic, P.S., Selemon, L.D., Schwartz, M.L., 1984. Dual pathways connecting the dorsolateral prefrontal cortex with the hippocampal formation and parahippocampal cortex in the rhesus monkey. *Neuroscience* 12, 719–743.
- Grave de Peralta, M.R., Gonzalez, A.S., Lantz, G., Michel, C.M., Landis, T., 2001. Noninvasive localization of electromagnetic epileptic activity. I. Method descriptions and simulations. *Brain Topogr.* 14, 131–137.
- Grill-Spector, K., Kushnir, T., Edelman, S., Itzhak, Y., Malach, R., 1998. Cue-invariant activation in object-related areas of the human occipital lobe. *Neuron* 21, 191–202.
- Guthrie, D., Buchwald, J.S., 1991. Significance testing of difference potentials. *Psychophysiology* 28, 240–244.
- Haxby, J.V., Ungerleider, L.G., Clark, V.P., Schouten, J.L., Hoffman, E.A., Martin, A., 1999. The effect of face inversion on activity in human neural systems for face and object perception. *Neuron* 22, 189–199.
- Hubel, D.H., Wiesel, T.N., 1962. Receptive fields, binocular interaction and functional architecture in the cat’s visual cortex. *J. Physiol.* 160, 106–154.
- Hupe, J.M., James, A.C., Payne, B.R., Lomber, S.G., Girard, P., Bullier, J., 2001. Feedforward and feedback connections between areas V1 and V2 of the monkey have similar rapid conduction velocities. *J. Neurophysiol.* 85 (3), 1328–1331.

- J., 1998. Cortical feedback improves discrimination between figure and background by V1, V2 and V3 neurons. *Nature* 20 (394(6695)), 784–787.
- Hupe, J.M., James, A.C., Girard, P., Lomber, S.G., Payne, B.R., Bullier, J., 2001. Feedback connections act on the early part of the responses in monkey visual cortex. *J. Neurophysiol.* 85 (1), 134–145.
- Kanwisher, N., McDermott, J., Chun, M.M., 1997. The fusiform face area: a module in human extrastriate cortex specialized for face perception. *J. Neurosci.* 17, 4302–4311.
- Kosslyn, S.M., Behrmann, M., Jeannerod, M., 1995. The cognitive neuroscience of mental imagery. *Neuropsychologia* 33, 1335–1344.
- Kovacs, G., Vogels, R., Orban, G.A., 1995. Selectivity of macaque inferior temporal neurons for partially occluded shapes. *J. Neurosci.* 15 (3 Pt. 1), 1984–1997.
- Lamme, V.A., Spekreijse, H., 2000. Modulations of primary visual cortex activity representing attentive and conscious scene perception. *Front Biosci.* 5, D232–D243.
- Lerner, Y., Hendler, T., Ben-Bashat, D., Harel, M., Malach, R., 2001. A hierarchical axis of object processing stages in the human visual cortex. *Cereb. Cortex* 11, 287–297.
- Logothetis, N.K., Pauls, J., Augath, M., Trinath, T., Oeltermann, A., 2001. Neurophysiological investigation of the basis of the fMRI signal. *Nature* 412, 150–157.
- Malach, R., Reppas, J.B., Benson, R.R., Kwong, K.K., Jiang, H., Kennedy, W.A., 1995. Object-related activity revealed by functional magnetic resonance imaging in human occipital cortex. *Proc. Natl. Acad. Sci. U. S. A.* 92, 8135–8139.
- Marr, D., Nishihara, H.K., 1978. Representation and recognition of the spatial organization of three-dimensional shapes. *Proc. R. Soc. Lond., B Biol. Sci.* 200, 269–294.
- Martinez, A., Anillo-Vento, L., Sereno, M.I., Frank, L.R., Buxton, R.B., Dubowitz, D.J., 1999. Involvement of striate and extrastriate visual cortical areas in spatial attention. *Nat. Neurosci.* 2, 364–369.
- Michel, C.M., Thut, G., Morand, S., Khateb, A., Pegna, A.J., Grave, d.P., 2001. Electric source imaging of human brain functions. *Brain Res. Brain Res. Rev.* 36, 108–118.
- Miyashita, Y., Hayashi, T., 2000. Neural representation of visual objects: encoding and top-down activation. *Curr. Opin. Neurobiol.* 10, 187–194.
- Molholm, S., Ritter, W., Javitt, D.C., Foxe, J.J., 2004. Multisensory visual–auditory object recognition in humans: a high-density electrical mapping study. *Cereb. Cortex* 14, 452–465.
- Murray, M.M., Foxe, J.J., Higgins, B.A., Javitt, D.C., Schroeder, C.E., 2001. Visuo-spatial neural response interactions in early cortical processing during a simple reaction time task: a high-density electrical mapping study. *Neuropsychologia* 39 (8), 828–844.
- Murray, M.M., Wylie, G.R., Higgins, B.A., Javitt, D.C., Schroeder, C.E., Foxe, J.J., 2002. The spatiotemporal dynamics of illusory contour processing: combined high-density electrical mapping, source analysis, and functional magnetic resonance imaging. *J. Neurosci.* 22, 5055–5073.
- Murray, M.M., Foxe, D.M., Javitt, D.C., Foxe, J.J., 2004. Setting boundaries: brain dynamics of modal and amodal illusory shape completion in humans. *J. Neurosci.* 24, 6898–6903.
- Murray, M.M., Molholm, S., Michel, C.M., Ritter, W., Heslenfeld, D.J., Schroeder, C.E., Javitt, D.C., Foxe, J.J., 2005. Grabbing your ear: rapid auditory–somatosensory multisensory interactions in low-level sensory cortices are not constrained by stimulus alignment. *Cereb. Cortex* 15 (7), 963–974.
- Nakamura, H., Gattass, R., Desimone, R., Ungerleider, L.G., 1993. The modular organization of projections from areas V1 and V2 to areas V4 and TEO in macaques. *J. Neurosci.* 13 (9), 3681–3691.
- Op de, B.H., Beatse, E., Wagemans, J., Sunaert, S., Van, H.P., 2000. The representation of shape in the context of visual object categorization tasks. *NeuroImage* 12, 28–40.
- Pasupathy, A., Connor, C.E., 1999. Responses to contour features in macaque area V4. *J. Neurophysiol.* 82, 2490–2502.
- Perrin, F., Pernier, J., Bertrand, O., Giard, M.H., Echallier, J.F., 1987. Mapping of scalp potentials by surface spline interpolation. *Electroencephalogr. Clin. Neurophysiol.* 66, 75–81.
- Petrides, M., Alivisatos, B., Frey, S., 2002. Differential activation of the human orbital, mid-ventrolateral, and mid-dorsolateral prefrontal cortex during the processing of visual stimuli. *Proc. Natl. Acad. Sci. U. S. A.* 99, 5649–5654.
- Rempel-Clower, N.L., Barbas, H., 2000. The laminar pattern of connections between prefrontal and anterior temporal cortices in the rhesus monkey is related to cortical structure and function. *Cereb. Cortex* 10, 851–865.
- Rossion, B., Gauthier, I., Tarr, M.J., Despland, P., Bruyer, R., Linotte, S., 2000. The N170 occipito-temporal component is delayed and enhanced to inverted faces but not to inverted objects: an electrophysiological account of face-specific processes in the human brain. *NeuroReport* 11, 69–74.
- Rousselet, G.A., Thorpe, S.J., Fabre-Thorpe, M., 2004. Processing of one, two or four natural scenes in humans: the limits of parallelism. *Vision Res.* 44, 877–894.
- Sary, G., Vogels, R., Orban, G.A., 1993. Cue-invariant shape selectivity of macaque inferior temporal neurons. *Science* 260, 995–997.
- Schendan, H.E., Kutas, M., 2002. Neurophysiological evidence for two processing times for visual object identification. *Neuropsychologia* 40, 931–945.
- Scherg, M., Picton, T.W., 1991. Separation and identification of event-related potential components by brain electric source analysis. *Electroencephalogr. Clin. Neurophysiol., Suppl.* 42, 24–37.
- Scherg, M., von Cramon, D., 1985. Two bilateral sources of the late AEP as identified by a spatio-temporal dipole model. *Electroencephalogr. Clin. Neurophysiol.* 62, 32–44.
- Schnider, A., Treyer, V., Buck, A., 2000. Selection of currently relevant memories by the human posterior medial orbitofrontal cortex. *J. Neurosci.* 20, 5880–5884.
- Schroeder, C.E., Mehta, A.D., Givre, S.J., 1998. A spatiotemporal profile of visual system activation revealed by current source density analysis in the awake macaque. *Cereb. Cortex* 8, 575–592.
- Schroeder, C.E., Mehta, A.D., Foxe, J.J., 2001. Determinants and mechanisms of attentional control over cortical neural processing. *Front. Biosci.* 6, D672–D684.
- Sehatpour, P., Zemon, V., Molholm, S., Mehta, A., Schwartz, T., Javitt, D.C., Foxe, J.J., 2004. Perceptual closure processes during object recognition: an intracranial investigation in humans. Program No. 824.14. 2004 Abstract Viewer/Itinerary Planner. Society for Neuroscience, Washington, DC. (Online).
- Simpson, G.V., Foxe, J.J., Vaughan, H.G. Jr., Mehta, A.D., Schroeder, C.E., 1995. Integration of electrophysiological source analyses, MRI and animal models in the study of visual processing and attention. *Electroencephalogr. Clin. Neurophysiol., Suppl.* 44, 76–92.
- Slotnick, S.D., Yantis, S., 2003. Efficient acquisition of human retinotopic maps. *Hum. Brain Mapp.* 18 (1), 22–29.
- Snodgrass, J.G., Corwin, J., 1988. Perceptual identification thresholds for 150 fragmented pictures from the Snodgrass and Vanderwart picture set. *Percept. Mot. Skills* 67, 3–36.
- Snodgrass, J.G., Feenan, K., 1990. Priming effects in picture fragment completion: support for the perceptual closure hypothesis. *J. Exp. Psychol. Gen.* 119, 276–296.
- Snodgrass, J.G., Vanderwart, M., 1980. A standardized set of 260 pictures: norms for name agreement, image agreement, familiarity, and visual complexity. *J. Exp. Psychol. Hum. Learn.* 6, 174–215.
- Spencer, K.M., Nestor, P.G., Perlmutter, R., Niznikiewicz, M.A., Klump, M.C., Frumin, M., Shenton, M.E., McCarley, R.W., 2004. Neural synchrony indexes disordered perception and cognition in schizophrenia. *Proc. Natl. Acad. Sci.* 7 (101(49)), 17288–17293.
- Talairach, J., Tournoux, P., 1988. *Co-Planar Stereotaxic Atlas of the Human Brain*. Thieme, New York.
- Tanaka, K., 1996. Inferotemporal cortex and object vision. *Annu. Rev. Neurosci.* 19, 109–139.

- Thompson-Schill, S.L., D'Esposito, M., Kan, I.P., 1999. Effects of repetition and competition on activity in left prefrontal cortex during word generation. *Neuron* 23, 513–522.
- Thorpe, S., Fize, D., Marlot, C., 1996. Speed of processing in the human visual system. *Nature* 381(6582), 520–522.
- Tulving, E., Schacter, D.L., 1990. Priming and human memory systems. *Science* 247, 301–306.
- Ullman, S., 1995. Sequence seeking and counter streams: a computational model for bidirectional information flow in the visual cortex. *Cereb. Cortex* 5, 1–11.
- Urbano, A., Babiloni, C., Onorati, P., Babiloni, F., 1996. Human cortical activity related to unilateral movements. A high resolution EEG study. *NeuroReport* 8, 203–206.
- Vecera, S.P., Farah, M.J., 1997. Is visual image segmentation a bottom–up or an interactive process? *Percept. Psychophys.* 59, 1280–1296.
- Viggiano, M.P., Kutas, M., 2000. Overt and covert identification of fragmented objects inferred from performance and electrophysiological measures. *J. Exp. Psychol.* 129 (1), 107–125.
- Wagner, A.D., Pare-Blagoev, E.J., Clark, J., Poldrack, R.A., 2001. Recovering meaning: left prefrontal cortex guides controlled semantic retrieval. *Neuron* 31, 329–338.
- Warnking, J., Dojat, M., Guerin-Dugue, A., Delon-Martin, C., Olympieff, S., Richard, N., Chehikian, A., Segebarth, C., 2002. fMRI retinotopic mapping—Step by step. *NeuroImage* 17 (4), 1665–1683.
- Zemel, R.S., Mozer, M.C., 2001. Localist attractor networks. *Neural Comput.* 13, 1045–1064.